

AD-A103 695

COLORADO UNIV AT BOULDER

F/G 7/4

VIBRATIONAL PRODUCT STATES FROM REACTIONS OF CN(-) WITH THE HYD--ETC(U)

JAN 81 M M MARICG, M A SMITH, C J SIMPSON

DAAG29-79-6-0012

ARO-16004.7-C

NL

UNCLASSIFIED

1 of 1
ADA
7-2000



END
DATE
FILMED
10-81
DTIC

Vibrational product states from reactions of CN^- with the hydrogen halides and hydrogen atoms

M. Matti Maricq,^{a)} Mark A. Smith, C. J. S. M. Simpson,^{a)} and G. Barney Ellison

Department of Chemistry, University of Colorado, Boulder Colorado 80309
and Joint Institute for Laboratory Astrophysics, University of Colorado, and National Bureau of Standards,
Boulder, Colorado 80309

(Received 15 January 1981; accepted 20 February 1981)

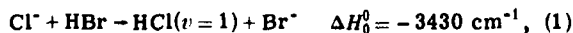
Infrared chemiluminescence is observed from the C-H stretch manifold ν_3 of HCN formed in the gas phase ion-molecule reactions: $\text{CN}^- + \text{HX} \rightarrow \text{HCN}(\nu_3) + \text{X}^-$, with (X = Cl, Br, I), and for $\text{CN}^- + \text{H} \rightarrow \text{HCN}(\nu_3) + e^-$. Qualitative information is also obtained for excitation in the bending mode. In each case some excitation is observed in the highest level allowed by energy conservation. Comparison with similar studies of the reactions $\text{Cl}^- + \text{HX}$ shows that the stretching mode of the newly formed bond is less efficiently populated in the HCN case. Emission is observed from CNH (hydroisocyanic acid) formed in the reaction $\text{CN}^- + \text{HI} \rightarrow \text{CNH}(\nu) + \text{I}^-$.

DTIC
ELECTE
SEP 2 1981
H

I. INTRODUCTION

Reaction mechanisms are increasingly viewed as problems in reaction dynamics.¹⁻⁵ A vast effort has been made in the study of neutral, radical reactions and this is steadily being extended to include ions.⁶⁻¹⁹ An important difference between neutral and ion reactions is the intermolecular potential. The potential between neutrals is only weakly attractive and generally features a barrier which must be surpassed for reaction to take place. In contrast, ion-molecule reactions feature potentials dominated by the attractive ion-dipole and ion-induced dipole terms and, consequently, pass through potential minima.^{11,12} How will this fundamental difference in potential energy surfaces affect the reaction dynamics? One method to investigate this question is to determine the deposition of energy among the reaction products. Many ion reactions are quite fast and have large exothermicities.⁷ It is likely that ion-molecule reaction products will be internally excited. If a pattern of energy disposal can be discerned, this information can be compared and contrasted to the wealth of data available for neutral reactions.

The reaction dynamics of ions has been studied in beams and reaction products have been observed in electronic emission spectroscopy.^{13,14} Recently, the first observation of infrared chemiluminescence from an ion-molecule reaction was reported from this laboratory.¹⁵ The flowing afterglow method¹⁶ was adapted by addition of an IR detection system to observe the vibrational fluorescence from the products of ion reactions. A complete study of the product vibrational energy distribution of HCl produced in the reactions of Cl^- with HBr and HI was subsequently carried out by Zwier *et al.*¹⁷



The results reported there demonstrated the usefulness of the technique for obtaining quantitative information

about the vibrational states of the nascent product molecule.

In this paper we would like to apply our infrared chemiluminescence technique to ion reactions that produce polyatomic (rather than diatomic) molecules as products. The study of IR emission from polyatomic species is much more complicated than processes such as Reactions (1) or (2). Instead of the excitation being in just one vibrational mode as in HCl, (3N-6) modes are available for an N atom species, (3N-5) if the molecule is linear. We would like to know which of the many internal modes are populated in a vibrationally excited polyatomic product born in an ion-molecule reaction. How much energy is deposited into a particular mode?

A host of problems accompany the study of emission from a polyatomic species. For instance, the spectroscopy of the molecule becomes more complicated and the emission lines may be difficult to sort out and assign. Worse yet, the energy may scramble via intramolecular pathways so that the resulting emission bears little resemblance to the initial product state distribution. In an extreme case, the internal energy may rapidly leak out by deactivation of a low frequency vibrational mode by collision with other species in the flow tube resulting in no emission at all.

As a first step in the study of polyatomic reaction products, we have chosen a triatomic molecule. This molecule must be selected to minimize the spectroscopic problems noted above and to meet certain requirements imposed by the flowing afterglow technique.

We selected HCN. This molecule has several attractive spectroscopic features:

(1) The first attraction is that the (ν_3) mode—the H-CN stretch—is well separated from the nearest energy levels. (The particular vibrational modes are labeled by ν_n while ν_n designates the number of quanta in mode ν_n . We adopt the notation ν_1 for the $\text{C}\equiv\text{N}$ stretch, ν_2 for the H-C-N bend, and ν_3 for the C-H stretch.) The result is that, as in the case of the $\nu_3=1$ state of CO_2 , a negligible amount of vibrational deactivation should be caused by collisions with the 0.3 Torr of He in the ob-

^{a)} Present address: Physical Chemistry Laboratory, South Parks Road Oxford, OX1 3QZ England.

AD A103695

81 9 01 106 DTIC FILE COPY

TABLE I. Reactions, rates and exothermicities.^a

Reaction	ΔH_0^0 kcal mol ⁻¹	ΔH_0^0 cm ⁻¹	k (experimental) cm ³ s ⁻¹	k (ADO) cm ³ s ⁻¹
CN ⁻ + HF → HCN + F ⁻	20.4	7 150
CN ⁻ + HCl → HCN + Cl ⁻	-17.7	-6 180	3.0(-9)	1.5(-9)
CN ⁻ + HBr → HCN + Br ⁻	-27.4	-9 600	2.4(-9)	1.3(-9)
CN ⁻ + HI → HCN + I ⁻	-36.7	-12 800	1.3(-9)	1.3(-9)
CN ⁻ + H → HCN + e ⁻	-36.5	-12 800	1.3(-9)	...
CN ⁻ + DI → DCN + I ⁻	-37.1	-13 000
Cl ⁻ + HBr → HCl + Br ⁻	-9.8	-3 430	7.5(-10)	...
Cl ⁻ + HI → HCl + I ⁻	-19.0	-6 650	6.3(-10)	...
Cl ⁻ + H → HCl + e ⁻	-18.9	-6 610	9.6(-10)	...

^aThe tabulated rate constants abbreviate the exponent; the constant for CN⁻ reacting with HCl is 3.0×10^{-9} cm³ s⁻¹. The average dipole orientations approximation (ADO) is taken from Ref. 63. The rate constant for CN⁻ + H is taken from Fehsenfeld (Ref. 47) while Zwier *et al.* (Ref. 17) have supplied data for the last three Cl⁻ reactions. The uncertainty in ΔH_0^0 for all of the CN⁻ reactions is ± 2.6 kcal mol⁻¹ or ± 900 cm⁻¹.

servation time of about 0.5 msec.¹⁸⁻²⁰

(2) The H-CN band emits strongly, having an intensity about twice that of HCl. This is crucial in order that the IR chemiluminescence can be detected.

(3) One major advantage of studying HCN instead of, say, CO₂ is that the ν_3 mode of HCN is very anharmonic, being about 100 cm⁻¹. This anharmonicity is greater than the rotational-vibrational envelope of the band. So it will be possible to separate emission from, say, the (003)-(002) transition and that of (002)-(001) using interference filters. This is not possible for the (00_n) levels of CO₂.

The ion-molecule reactions which are the subject of this paper are the proton abstraction reactions



and the associative detachment reaction



This set of reactions has several attractive features.

(1) Reactions (3)-(6) are all very fast and proceed on about every collision as shown in Table I.

(2) The reagent ion CN⁻ can be produced in large quantities (ion densities of 10⁸ cm⁻³) from several different precursors.

(3) Any reactions involving neutral CN radicals will be regigibly slow²¹ compared with those of CN⁻.

We report in this paper the relative populations of HCN(00 ν_3) produced by the ion reactions (3)-(6). Table I shows the exothermicities of Reactions (3)-(6) are small enough to excite the H-CN stretch over the range ($\nu_3=1$) to ($\nu_3=4$). It is much more difficult to study the degree of excitation of the ν_1 and the ν_2 modes. By the appropriate use of deactivation and energy transfer techniques, we have obtained some information on the population in the bending mode.

A totally unexpected result is that the reaction be-

tween CN⁻ and HI produces CNH as well as HCN. HCN is the only product observed in the reaction of CN⁻ with H atoms even though Reactions (5) and (6) have about the same exothermicities (Table I). This is of great interest as CNH has been observed in interstellar space.²²⁻²⁴

II. EXPERIMENTAL

A summary of the experimental conditions used for the CN⁻ reactions is given here. A more complete description of the apparatus and tests on its performance is given in Ref. 17.

A. The flowing afterglow apparatus

The flowing afterglow apparatus used for the present experiments is depicted in Fig. 1. At the upstream end, helium (or argon) carrier gas enters via the ionizer assembly. Electron impact produces helium ions, metastables, and slow electrons which subsequently react with the reagents introduced through the ion precursor inlet to produce reactant ions. The mixture is allowed to flow downstream for approximately 40 cm before the addition of the neutral reagents; the flow velocity of the buffer gas is 8×10^3 cm s⁻¹. This corresponds to about 2×10^4 collisions with the He buffer gas, allowing for the establishment of clean flow conditions and the completion of the reactions producing the desired ions. This large number of collisions tends to thermally equilibrate the ions. Neutral reagents can be admitted either through the radial inlets or the movable injector. Both provide for a uniform addition of the reagent across the cross section of the flow tube which in turn allows us to characterize the time origin for the reaction. The ions are then sampled through the nose cone which has a 0.25 mm orifice and is held at +3 V to attract the negative ions. Finally mass analysis is achieved with a quadrupole mass filter and the ions are detected either with a ceratron particle counter or by measuring the current on a Faraday plate.

B. Infrared detection

The usual flowing afterglow apparatus¹⁶ has two modifications to allow for the detection of infrared chemiluminescence. One is an observation window normal to the direction of flow which is installed near the down-

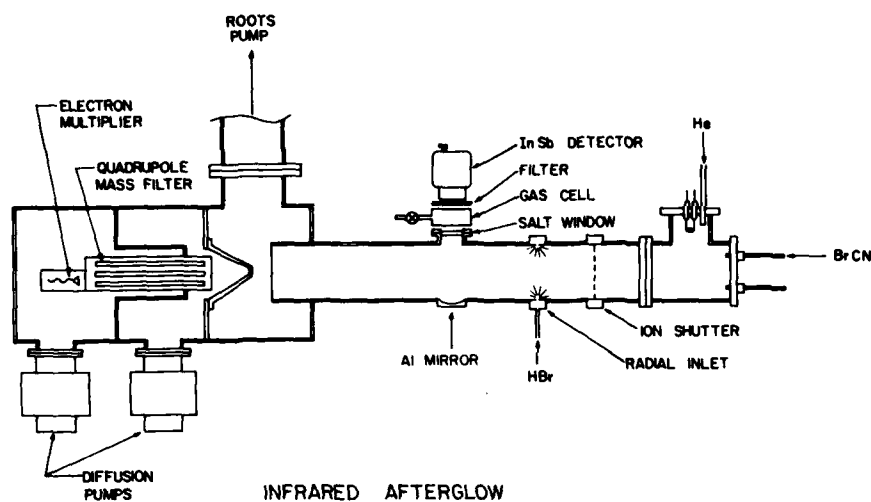


FIG. 1. A schematic of the flowing afterglow apparatus.

stream end of the flow tube. The window is placed roughly tangent to the inside wall of the flow tube (about 4 cm from the axis). This allows light collection from a large volume and hence improves the signal-to-noise ratio. A 10 cm focal length aluminum mirror lies opposite the window to further increase light gathering. In practice neutral inlets at various distances from the window are used to allow emission signals to be recorded at different times from the origin of the reaction.

The second modification is the placement of a tungsten mesh across the flow tube upstream of the neutral inlets. This is the ion shutter shown in Fig. 1. A potential of about 10 V applied to the mesh interrupts the flow of ions. Square wave modulation of the potential (0–10 V, 200 Hz) on the mesh results in the formation of packets of ions, thus modulating the products of ion reactions. Since neutral reactants will not be affected, this method enables us to distinguish emission of products of ion-molecule reactions from background emission. This modulation technique is crucial to our experiment as the electron impact source also produces excited neutral species which can react with constituents present in the flow tube. Use of these voltages on the tungsten mesh achieved about 50% modulation of the ions. Higher mesh voltages may cause electron detachment from the negative ions at the ion shutter. The emission signals reported in this paper did not depend on the mesh voltage, modulation frequency, or duty cycle, in the region near the values used.

A 1.27 cm diam 77 K InSb detector was used in conjunction with a set of interference filters to resolve and detect infrared emission. The output from the InSb detector was amplified and signal averaged. The resulting modulated waveform was then integrated to improve the signal-to-noise ratio and displayed on an X-Y recorder. A representative IR emission spectrum is shown in Fig. 2; the signal is from $\text{HCN}(00n)$ where $n=1, 2,$ and 3 . The HCN is produced by reaction of CN^- with HBr . In this experiment the ions are stopped by the ion shutter at $t=0$. Subsequent depletion of the excited reaction products appears as a decrease in the IR signal at $t=2$ or 3 msec. The integral of the dip in the IR signal is

also displayed. The increased signal-to-noise ratio is evident.

C. CN^- production

One of the requirements for detection of vibrational chemiluminescence from products of ion-molecule reactions is to begin with very high densities of reactant ions (about 10^8 cm^{-3}). This corresponds to roughly four orders of magnitude higher densities than is typical in standard flowing afterglow experiments. Not all precursor reagents provide the required number of ions. The CN^- must also be the only reactive ion present in the flow tube. Any other ions, positive or negative, which undergo reactions could produce interfering sources of emission.

Two molecules were used as precursors to CN^- —cyanogen (C_2N_2) and cyanogen bromide (BrCN). Neither was perfect; however the chemiluminescence results obtained did not depend on which reagent was used. About 1 or 2 pA of ion current (CN^- at $m/z=26$) was measured

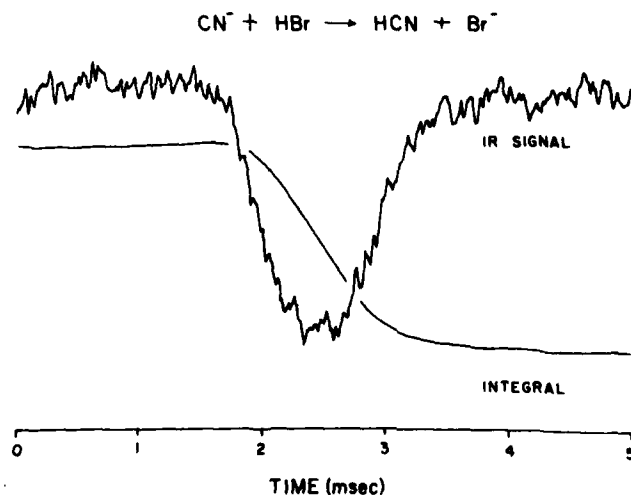


FIG. 2. A typical IR emission signal and its integral in the 3000 cm^{-1} region after 10 min of signal averaging.

on the Faraday plate when C_2N_2 was used as the ion source. This was sufficient to observe a reasonable emission signal from HCN after 128 K sweeps (roughly 10 min of signal averaging). The only negative ion produced from C_2N_2 is CN^- . The positive ion spectrum is rather complex consisting of C_2N_2^+ , C_2N_4^+ , C_4N_4^+ , and so on to high mass polymeric ions. As HCl is added to the flow tube, CN^- disappears and Cl^- appears indicating that Reaction (3) occurs. Since this reaction is very fast, only small flows (low pressures) of HCl are required to achieve complete reaction in the 5–11 cm before the IR detector (a throughput Q of 1 STP $\text{cm}^3 \text{s}^{-1}$ or 2.3 mTorr was sufficient). No reactions of the positive ions were observed when HCl was added to the apparatus with C_2N_2 as the ion precursor. However, both HBr and HI react with C_2N_2 positive ions. This is an undesirable situation since such reactions may produce emitting species which will be modulated.

Cyanogen bromide (BrCN) was used as a second source of CN^- . BrCN produces about four times as much CN^- ions as cyanogen. Unfortunately, CN^- is not the only negative ion produced; about 10% of the total negative ion intensity is Br^- . Although Br^- is only a small fraction of the negative ions present, its reactions with HI and H will result in vibrationally excited HBr (the analogous reactions with HCl and HBr are not exothermic). Emission from $\text{HBr}(v)$ can be excluded by using a fixed frequency filter which blocks light below 2800 cm^{-1} .

The positive ion spectrum produced by BrCN consists of three sets of peaks due to Br^+ , HCNBr^+ , and CNBr_2^+ . Addition of any reagent (HCl, HBr, HI) causes the CNBr_2^+ peak to decrease and the HCNBr^+ peak to increase. Furthermore, IR radiation can easily be de-

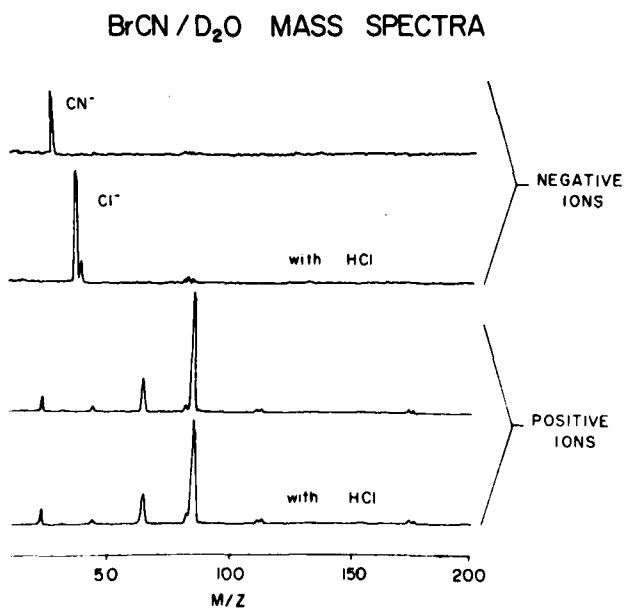


FIG. 3. Mass spectra of both positive and negative ions in the flow tube before and after addition of HCl reactant gas. D_2O is present (0.2 mTorr) to ensure that the only change in the spectra is from the desired negative ion-molecule reaction.

TABLE II. Neutral reactions with CN^- .

	ΔH_0^0 kcal mol $^{-1}$	ΔH_0^0 cm $^{-1}$	k cm $^3 \text{s}^{-1}$
$\text{CN} + \text{HF} \rightarrow \text{HCN} + \text{F}$	10.7	3750	...
$\text{CN} + \text{HCl} \rightarrow \text{HCN} + \text{Cl}$	-22.4	-7830	3.7(-14)
$\text{CN} + \text{HBr} \rightarrow \text{HCN} + \text{Br}$	-38.0	-13300	3.7(-13)
$\text{CN} + \text{HI} \rightarrow \text{HCN} + \text{I}$	-54.2	-19000	7.6(-12)

*Rate constants were measured by G. Roden (Ref. 21).

tected without the addition of any neutral reagent whatsoever. The use of filters enabled us to narrow the frequency range of the emission to 3200–3400 cm^{-1} and 1800–2000 cm^{-1} . It was noted that upon the addition of D_2O to the flow tube, DCNBr^+ was present in the flow tube instead of HCNBr^+ . Concurrently, the IR emission shifted into the 2200–2500 cm^{-1} range. We attribute the IR signals to emission from the C–H stretch and $\text{C}\equiv\text{N}$ stretch of HCNBr^+ . Addition of D_2O to the system shifts the interfering IR signals to a region of the spectrum where they can be conveniently blocked with the appropriate filter.

Consequently, about 0.2 mTorr of D_2O was added to the flow tube upstream from the neutral inlets for the majority of the experiments in which BrCN was used as a precursor to CN^- . The positive ion mass spectrum then consisted entirely of the clusters $\text{D}_3\text{O}^+(\text{D}_2\text{O})_n$ and was unaffected by the addition of any neutral reactants. The mass spectra for both positive and negative ions produced in the mixture BrCN/ D_2O are displayed in Fig. 3. A filter which cut off below 2800 cm^{-1} was always used when emission from vibrationally excited HCN was examined. In several instances (notably in the energy transfer studies to OCS and for the reaction of CN^- with DI) when emission was expected below 2800 cm^{-1} , H_2O was added to the flow tube and blocking filters above 3000 cm^{-1} were employed.

Although the addition of D_2O solves the problem of interfering emission due to positive ion reactions, it is important to determine if D_2O will vibrationally deactivate the newly formed HCN. In practice the pressure of D_2O was 1000 times lower than that of the He buffer gas. The nascent HCN would suffer fewer than five collisions with D_2O before being observed at the IR detector; this suggests that deactivation by D_2O will not be a problem. The same relative emission intensities were observed using C_2N_2 or BrCN as the source of CN^- , so neither the positive ion chemistry in C_2N_2 nor the addition of D_2O to BrCN affects emission.

The CN^- ions which might be detached by the mesh voltage form a modulated source of CN. These may react to form vibrationally excited HCN. Vibrational emission due to a similar mechanism was observed by Zwier *et al.*¹⁷ The rates of reaction of CN are roughly 3 to 4 orders of magnitude slower than those of the ion-molecule reactions as shown by the rate constants²¹ listed in Table II. This implies that a detectable quantity of "radical-generated" HCN cannot be produced in the time available. There is no effect on the IR signal as the mesh voltage is increased. Hence radical reac-

TABLE III. Spectroscopic information for HCN and CNH.

$$\nu = E - E_0 = \omega_1^0 \nu_1 + \omega_2^0 \nu_2 + \omega_3^0 \nu_3 - X_{11} \nu_1^2 - X_{22} \nu_2^2 - X_{33} \nu_3^2 - X_{12} \nu_1 \nu_2 - X_{13} \nu_1 \nu_3 - X_{23} \nu_2 \nu_3 - g_{22} l^2.$$

	HCN ^a		CNH		CND	
	(cm ⁻¹)	(cm ⁻¹)	Gas phase frequencies (cm ⁻¹)	Ar matrix frequencies (cm ⁻¹)	Gas phase frequencies (cm ⁻¹)	Ar matrix frequencies (cm ⁻¹)
ω_1^0	2107.06	1932.37	ν_1 ...	2029.	...	1940.
ω_2^0	710.77	569.22	ν_2 ...	477.	...	374.
ω_3^0	3363.90	2650.56	ν_3 3652.9	3620.	2780.4	2769.
X_{11}	10.45	7.10	B_0 1.51211		1.27264	
X_{22}	2.50	2.09				
X_{33}	52.50	20.23				
X_{12}	2.90	-2.73				
X_{13}	14.43	32.88				
X_{23}	19.19	15.71				
B_0	1.47791	1.20770				
g_{22}	-3.63	-2.00				

^aInfrared Absorbance Intensities:for HCN: $S_1 = 1 \text{ atm}^{-1} \text{ cm}^{-2}$; $S_2 = 257 \text{ atm}^{-1} \text{ cm}^{-2}$; $S_3 = 238 \text{ atm}^{-1} \text{ cm}^{-2}$.for DCN: $S_1 = 13 \text{ atm}^{-1} \text{ cm}^{-2}$; $S_2 = 68 \text{ atm}^{-1} \text{ cm}^{-2}$; $S_3 = 121 \text{ atm}^{-1} \text{ cm}^{-2}$.

tions are of no consequence for the present study.

Electronic grade HCl (99.9%), high purity HBr (99%), HI (98%), and OCS (97.5%) were obtained from Matheson and used without further purification (except for the HI used in the kinetics measurements which was purified to remove H₂). He carrier gas was passed through a liquid nitrogen cold trap before being used. Cyanogen (Matheson 98.5%) was used without purification while cyanogen bromide (Aldrich 97%) was distilled from sodium prior to use. HCN was prepared from sodium cyanide and sulfuric acid.²⁵ Hydrogen atoms were produced in a thermal dissociator by passing high purity H₂ over a hot tungsten filament in a water cooled glass chamber which had been coated with boric acid (alternatively halocarbon wax²⁶) to inhibit surface recombination.²⁷

III. HCN PROPERTIES

A. Thermochemistry

The amount of energy available for internal excitation of product HCN formed in Reactions (3)–(6) depends on the exothermicities of these reactions. These quantities are calculated using Eq. (7) and are listed in Table I:

$$\Delta H_0^0 = EA(\text{CN}) - D_0^0(\text{H-CN}) + D_0^0(\text{HX}) - EA(\text{X}). \quad (7)$$

The electron affinity of CN is obtained from the photoionization²⁸ of HCN and is $EA(\text{CN}) = 3.82 \pm 0.02 \text{ eV}$. The dissociation energy $D_0^0(\text{HCN}) = 5.40 \pm 0.09 \text{ eV}$ and is calculated from the heats of formation²⁹ of HCN, H, and CN. The dissociation energies of the hydrogen halides can be obtained from Huber and Herzberg³⁰ while the electron affinities of the halide ions are available from Hotop and Lineberger.³¹ The energies of the reactions are listed in Table I.

Exothermicities for the same reactions producing CNH will differ by the relative stability of CNH versus HCN. This energy gap has been calculated by several groups^{32,33} but only sketchy experimental data are available.³⁴ A reasonable figure for this isomerization energy is about 15 kcal mol⁻¹ or 0.63 eV.³³ Thus roughly 5200 cm⁻¹ less energy is available for internal excitation of CNH than for HCN in all of these reactions. Only reactions of CN⁻ with HI and H should release enough energy to produce vibrationally excited CNH.

B. Spectroscopy

The values of the spectroscopic constants for HCN and DCN are available from Allen *et al.*³⁵ A table of these is provided for convenience (Table III). The three fundamental frequencies are $\nu_1 = 2096.6$, $\nu_2 = 708.3$, and $\nu_3 = 3311.4 \text{ cm}^{-1}$. Important values for the present experiments are the anharmonicity, $X_{33} = 52.5 \text{ cm}^{-1}$ and the rotational constant, $B_e = 1.48 \text{ cm}^{-1}$. A large anharmonicity factor for the C–H stretch in comparison to a relatively modest rotation constant indicates that emission from the sequence levels in this mode may be separable by the use of narrow bandpass filters. Although the *P* lines of one transition overlap with the *R* lines of the next, a deconvolution procedure is possible. Note that the anharmonicity factor of $X_{22} = 2.5 \text{ cm}^{-1}$ makes a similar prospect impossible for the bending mode ν_2 under present experimental conditions. This problem also exists for the C≡N stretch ν_1 .

The infrared intensities for the modes of HCN have been measured by Kim and King.³⁶ Their values are reported in Table III. Note that the absorption intensities³⁷ for the C–H stretch and the bend are reasonably large: 238 atm⁻¹ cm⁻² and 257 atm⁻¹ cm⁻², respectively, (com-

pared to 174 atm⁻¹ cm⁻² for HCl³⁸). Unfortunately, the very small value for the C≡N stretch (ν_1) will make it impossible to observe direct emission from this mode. As mentioned earlier, the small anharmonicity constant will not allow us to separate the emission from the various levels of the bend ν_2 . In addition, though the absorption strength is about the same, the Einstein A coefficient varies as ν^3 so that the IR emission from the bending mode can be expected to be smaller by a factor of 0.05 than the emission from the C-H stretch. Consequently, it was not surprising that no signal could be detected in the 700 cm⁻¹ region.

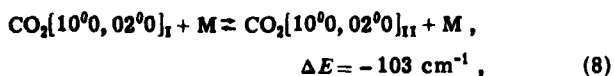
The infrared spectrum of CNH was first obtained by Milligan and Jacox³⁹ who photolyzed methyl azide in an argon matrix. Gas phase emission spectra were obtained by Arrington and Ogryzlo⁴⁰ for CNH and CND but only for the ν_3 mode. At 3653 cm⁻¹, the N-H stretch can be easily distinguished from the C-H stretch with our interference filters. The other spectral constants are collected in Table III.

We must know how intense CNH infrared emission is. We can estimate the absorption strength of the ($\nu_3 = 1$) - ($\nu_3 = 0$) of CNH relative to the same transition in HCN. This can be done by calculating the ratio of the respective Einstein A coefficients $A_{001}(\text{CNH})/A_{001}(\text{HCN})$. Our value for this ratio is based on an *ab initio* GVB(PP) calculation of the dipole moment derivatives for both HCN and CNH. These computations were carried out by Dr. J. J. Wendoloski of the NRCC and are outlined in Appendix A. He finds the ratio $A_{001}(\text{CNH})/A_{001}(\text{HCN})$ to be 4.0. Hence, emission from the N-H stretch of CNH should be roughly four times as bright as emission of the C-H stretch of HCN.

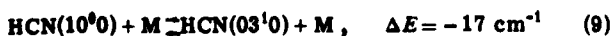
C. Vibrational relaxation of HCN

HCN is a triatomic molecule in which vibrational relaxation is expected to be similar to that of CO₂. The most important difference is that in energy relaxation experiments with CO₂, collisions between CO₂ molecules play an important role in holding the bending and stretching levels in equilibrium. In contrast, these flowing afterglow experiments have the concentration of HCN molecules so low that there are no HCN-HCN collisions between the time of formation of the HCN and the observation of the IR emission.

In the case of CO₂, the bending and stretching levels are in Fermi resonance and are connected by very fast collisional processes such as



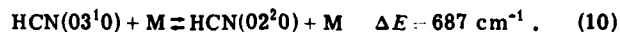
with k_9 being about $1 \times 10^5 \text{ sec}^{-1} \text{ Torr}^{-1}$ for He and varying little with the collision partner.⁴¹ The (100) state of HCN is Σ^+ , whereas the states (03¹0) and (03³0) are Π and Φ , respectively. Even though these states are nearly degenerate, there is no Fermi coupling as they have different symmetries. However, the process



is a dipole allowed transition with a very small energy

defect. It is expected to be very fast and to equilibrate the (10⁰0) and (03¹0) levels before the newly formed HCN is detected. This energy transfer [Reaction (9)] will be discussed in Sec. IV G.

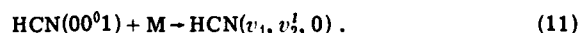
In the present experiment, deactivation will have to occur by processes such as



It is not known how fast these processes will occur for HCN. By analogy with the deactivation of the (01¹0) level of CO₂ at 667 cm⁻¹, one might expect that such a process would take about 1 msec with 0.3 Torr of He, about 10 msec with 0.3 Torr of Ar, and about 0.1 msec with this pressure of H₂.^{42,43}

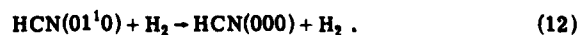
Clearly this argument applies to whether the (01¹0) mode will be retained, or collisionally deactivated before it can be observed. In fact, this analogy holds quite well and it proved to be possible either to retain or to deactivate the bending mode before the observation time by a judicious choice of carrier gas. Recall that it takes about 0.5 msec for the product HCN molecules to travel downstream to the InSb IR detector.

The (00⁰1) mode of CO₂ is relaxed very differently from the (01¹0) mode of CO₂; energy transfer probably taking place principally to the (11¹0) level which is 270 cm⁻¹ away. Unlike the relaxation of the (01¹0) level, that of the (00⁰1) level does not depend greatly on the collision partner.⁴⁴ An analogous process is to be expected for HCN with



If the level concerned is the (11¹0) or the (040), ΔE is about 500 cm⁻¹ exothermic; if it is the (050), the ΔE is about 200 cm⁻¹ endothermic. Considering that a vibration involving H is concerned but the energy gap is rather larger than in CO₂, values for k_{11} in the region of 200 sec⁻¹ Torr⁻¹ would be anticipated. McGarvey *et al.*⁴⁵ gave the rate constant as $< 100 \text{ sec}^{-1} \text{ Torr}^{-1}$ for M equals Ar or He and $< 200 \text{ sec}^{-1} \text{ Torr}^{-1}$ for M = H₂, while the recent work of Peterson and Smith¹⁹ gave $k_{11} = 250 \pm 30 \text{ sec}^{-1} \text{ Torr}^{-1}$ for both Ar and He.

Using the higher rate constant for M = He, we see that about 10% of the (00⁰1) level of HCN may be deactivated by He between the point of its formation and when we observe it. This is within our experimental error. The figures for M = H₂ are a good indication that adding a judicious amount of H₂ will deactivate the (01¹0) vibration while having a negligible effect on the (00¹) level. This has proved to be the case, since



We do not have information on the relaxation of CNH. We expect a similar picture to that of HCN with the H-NC stretch readily observable just as is the H-CN stretch.

IV. RESULTS

Ideally, it would be desirable to obtain a complete description of the vibrational state distribution for HCN produced by Reactions (3)-(6). Unfortunately, even for

this triatomic, such an endeavor is not possible with the present apparatus. However, a number of interesting results can be obtained when qualitatively different modes are available in the exit channel of the reaction.

(1) The relative populations of the ν_3 mode of product HCN molecules in Reactions (3)–(6) are determined.

(2) Considerable excitation in the HCN bending mode ν_2 is observed.

(3) Hydroisocyanic acid CNH is detected as a reaction product.

(4) Order of magnitude rate constants for the deactivation of $\text{HCN}(01^10)$ by He, Ar, and H_2 are found.

(5) Reaction rate constants for $\text{HX} + \text{CN}^- \rightarrow \text{HCN} + \text{X}^-$ are presented.

(6) Energy transfer from $\text{HCN}(v)$ to OCS is observed.

A. Analysis of data

Before embarking on a discussion of the findings, we present a brief description of the analysis by which the results are extracted.

Frequency selectivity in these experiments was obtained by using fixed interference filters which had a bandpass width of roughly 150 cm^{-1} and by the use of a 5 cm path length gas cell filled with 10 Torr of HCN. Figure 1 shows this gas cell placed between the observation window and the InSb IR detector. This will be referred to as the cold gas cell.

The anharmonicity of the C–H stretching mode depends also on the number of quanta in the bending mode through the term X_{23} (19 cm^{-1} as shown in Table III). Thus, with an appreciable number of quanta in ν_2 , this contribution from the cross term is comparable to that from the term X_{33} . Under the conditions of our experiment, the bending vibrations were shown to be relaxed before the observation station using helium and helium/hydrogen mixtures as carrier gases. In these circumstances, contributions from the X_{23} cross term do not arise. The sequence bands in ν_3 of HCN are separated by an amount Δ . This can be evaluated from Table III, $\Delta = 2X_{33}$ as 105 cm^{-1} . Thus, the filters used allow us to separate the transitions of $\text{HCN}(v_3 + 1) - \text{HCN}(v_3)$, where $v_3 = 3, 2, 1$, or 0. (We specify only v_3 when the quantum numbers of ν_1 and ν_2 are irrelevant.)

The use of fixed frequency interference filters can best be described by an example, say Reaction (3). Table I indicates that 6200 cm^{-1} ($\pm 900 \text{ cm}^{-1}$) is available to be partitioned into translational energy or rotation–vibration excitation of HCN. Consider first the emission intensity observed under deactivating circumstances when ν_1 and ν_2 are relaxed. In this case the only states of HCN which are possible are (00^00) , (00^01) , and (00^02) . If $N(001)$ is the number of HCN molecules in the (00^01) state within view of the InSb detector and $A(001)$ is the corresponding Einstein A coefficient, the integrated intensity I is

$$I = A(001)N(001) + A(002)N(002).$$

When a fixed frequency filter (say filter f) is placed

before the InSb detector, the observed intensity $I(f)$ is smaller:

$$I(f) = T(f, 1)A(001)N(001) + T(f, 2)A(002)N(002).$$

The T coefficients characterize the filter, i. e., $T(f, 2)$ is the fraction of the $(00^02) - (00^01)$ intensity transmitted by filter f . In general the amount of light passing through a filter f can be written

$$I(f) = \sum_{v_3} T(f, v_3)A(00v_3)N(00v_3).$$

If the ν_1 and ν_2 modes are not relaxed, the summation must be extended to include them. We can write this as

$$I(f) = \sum_{v_3} T(f, v_3)A(v_3)N(00v_3). \quad (13)$$

The quantity $A(v_3)$ is just the ratio of the spontaneous emission coefficients for the transition $(v_3) - (v_3 - 1)$ to that for $(1) - (0)$. The ratios $A(v_3)$ are discussed in Appendix A.

Knowing the transmission functions $T(f, v_3)$ for a set of filters and the Einstein coefficients, we measure $I(f)$ and invert Eq. (13) to find $N(00v_3)$. The normalization of the $N(00v_3)$ is arbitrary. We must measure the intensity with as many different filters as the maximum excitation of v_3 . In our case this implies that four filters are required for the most exothermic reaction (5). It should be pointed out that the numbers obtained via the above analysis are expected to be accurate to $\pm 25\%$. A major source of error is the accuracy of the angle dependence of the transmission through the filters.

The transmission of each rotational line of the $v_3 - v_3 - 1$ transition through each filter must be computed in order to construct the transmission coefficients, $T(f, v_3)$. A complication arises from the large solid angle of light collected by our detector. Although advantageous for signal to noise, this has the drawback of distorting the transmission curves for the filters because the transmission depends on the angle of incidence of the incoming light. Increasing the angle from the normal to the filter shifts its transmission to higher frequencies. The relation of the magnitude of this shift to the angle of incidence for our interference filters has been experimentally determined on a Beckman IR 12. Additional data are provided by OCLI.⁴⁶ It then remains to calculate the amount of light as a function of the angle of incidence.

The transmission of the band $(v_3) - (v_3 - 1)$ through a given filter is a sum over rotational states averaged over the collection angle θ :

$$T(f, v') = \int_0^{\theta_m} \rho(\theta) d\theta \left\{ \sum_J \frac{(2J+1)}{Q_R} \times \exp[-F_{v', J}/kT] [T(f, \nu_p, \theta) + T(f, \nu_R, \theta)] \right\}. \quad (14)$$

$F_{v', J}$ is the rotation energy of the upper state; $F_{v', J} = B_{v', J}(J+1)$. The function $T(f, \nu, \theta)$ is the transmission at frequency ν for light at an incident angle θ through the filter f . The transition frequencies are given by

$\nu = \nu_0 + (B_{\nu'} + B_{\nu''})m + (B_{\nu'} - B_{\nu''})m^2$, where m is $(J+1)$ for an R branch (ν_R) but m is $(-J)$ for a P branch (ν_P). $\rho(\theta)$ is the weighting function for photons arriving at angle θ to the normal. The exponential factor accounts for a Boltzmann distribution of rotational energy; Q_R is the rotational partition function. J varies over the rotational levels of the upper state. There are, thus, two frequencies for each J ; one for $\Delta J = 1$ (ν_R) the other for $\Delta J = -1$ (ν_P). For our detector $\theta_m = 40^\circ$ (half the angle of the cone of light collected). Transmission functions for various filters and for $\nu = 1$ to $\nu = 4$ were calculated numerically on a small digital computer. The filters we employed, together with their bandwidths and transmission functions, are tabulated in Appendix B.

Cold gas filter experiments were run under both deactivating and nondeactivating conditions; in one instance the buffer gas in the flow tube was H_2 and He but in the other only Ar. In the former case any state (v_1, v_2, v_3) is relaxed via collisions with H_2 to $(0, 0, v_3)$. The cold gas cell will then filter out the $(001) \rightarrow (000)$ transition from the overtones. The ratio of intensities through the gas cell (I_g) versus the empty gas cell (I_e) is given by

$$\frac{I_g}{I_e} = \frac{N(002)A(2) + \dots + N(00v_3)A(v_3)}{N(001) + N(002)A(2) + \dots + N(00v_3)A(v_3)} \quad (15)$$

Under nondeactivating conditions (Ar as the buffer gas) both the numerator and denominator of Eq. (15) must include terms of the form $N(v_1, v_2, v_3)A(v_3)$ arising from the contribution to the emission signals from combination bands. This means that the cold gas cell will be less effective as the states such as (011) will now pass through the gas cell, whereas if the bend were deactivated first, the emission would be blocked. The com-

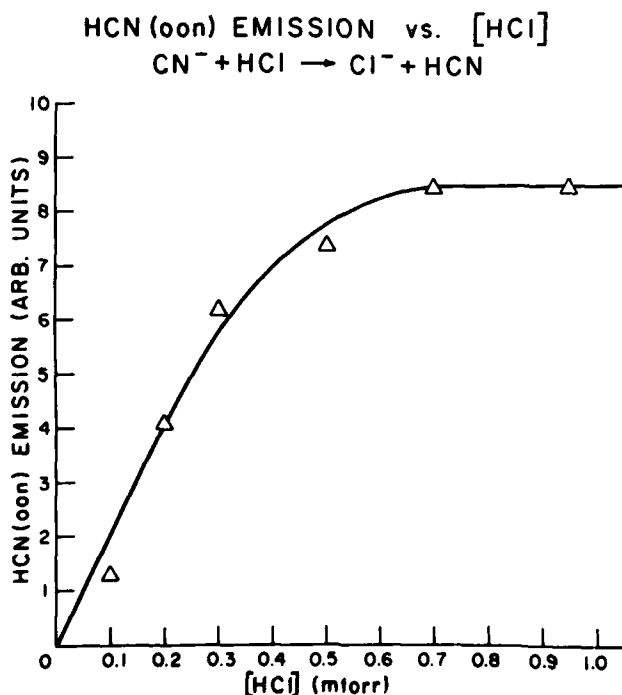


FIG. 4. Emission from the ν_3 mode of product HCN as a function of HCl pressure.

HCN(ν_3) EMISSION vs. CN^-
 $\text{CN}^- + \text{HCl} \rightarrow \text{Cl}^- + \text{HCN}$

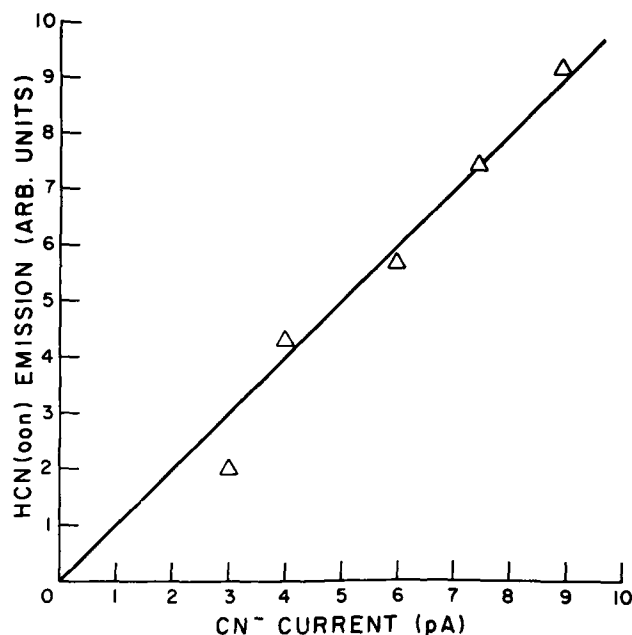


FIG. 5. HCN ν_3 emission as a function of total CN^- available for reaction.

parison of the effectiveness of the cold gas filter with and without deactivation thus gives us a measure of the amount of excitation in the bending mode.

B. $\text{CN}^- + \text{HCl}$

We will describe in some detail the extraction of relative populations in the H-CN stretch by using Reaction (3) as an example.

Vibrational emission from the 3300 cm^{-1} region was observed when HCl was added through the neutral inlet. Several checks were made to ensure that this signal was from the ion-molecule reaction (3). One was to see that the emission intensity grew linearly with the pressure of HCl and, then, saturated as CN^- was exhausted. Figure 4 depicts this behavior. Another check revealed that the emission signal scaled linearly with the amount of CN^- generated in the presence of a saturating pressure of HCl. This is shown in Fig. 5. Possibilities of other ion reactions in the flow tube are discussed above.

The exothermicity of Reaction (3) at 6200 cm^{-1} limits the number of accessible HCN vibrational states to 92. Recall that the uncertainty in ΔH_0° is 900 cm^{-1} so this number of 92 is not precise. Note the difference as compared¹⁷ to the two vibrational states available for HCl formed by $\text{Cl}^- + \text{HI}$. The rapid increase in numbers of states is perhaps the most prominent feature of the change from diatomic to polyatomic. CNH states are not considered for Reaction (3) as CNH(000) is just barely available with the energy released in the reaction. A simplified diagram of the ν_3 manifold for HCN

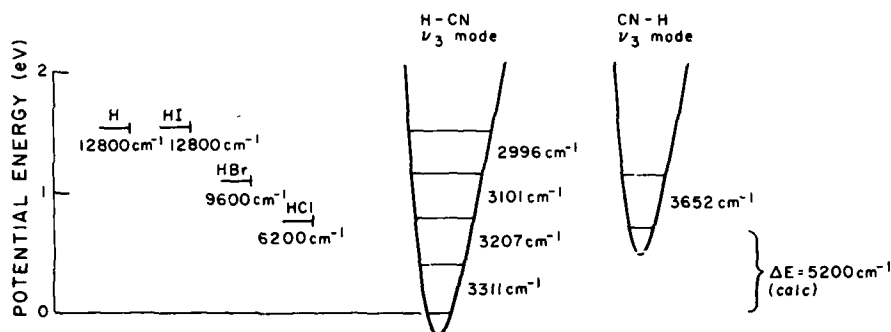


FIG. 6. Potential wells for the ν_3 mode of both HCN and CNH indicating their estimated relative stabilities. The experimentally determined vibrational splittings are indicated for both HCN and CNH. Also indicated are the exothermicities for Reactions (3)–(6).

and CNH is presented in Fig. 6. At the left of the diagram HCl is positioned 6200 cm^{-1} above $\nu=0$ of HCN. The 900 cm^{-1} error bars are indicated in Fig. 6 which suggest that there is some chance to produce $\text{HCN}(00^02)$.

The large number of available states reflects the various levels of excitation in the bending manifold. These can be eliminated by deactivation by addition of H_2 to the flow tube. With ν_2 now 0, six states then remain: (00^00) , (00^01) , (00^02) , (10^00) , (20^00) , and (10^01) . Collision with the buffer gas reaction (9) may equilibrate the $\text{C}\equiv\text{N}$ stretch with the bend manifold so that H_2 collisions should also remove any excitation in ν_1 . Only three states now remain: $\nu_3=0, 1$, or 2 . We have no direct measure of the population of HCN with $\nu_3=0$. The cold gas filter gives the ratio $I_g/I_e=0.19\pm 0.02$. Inverting Eq. (15), which now contains only two terms, we have

$$\frac{N(002)}{N(001)} = \frac{I_g/I_e}{[1 - (I_g/I_e)]A(2)} \quad (16)$$

This produces a population ratio $N(002)/N(001)$ of 0.11 ± 0.03 .

As mentioned earlier, there is a correction to this ratio due to the deactivation of the C–H stretch by He and H_2 . Additionally, a correction should be considered for the loss of energy from the ν_3 mode by radiative cascading. Both of these can be combined into

$$\frac{d}{dt} \mathbf{N}_t = \Gamma \mathbf{N}_t, \quad (17)$$

where $\mathbf{N}_t = [N(2), N(1), N(0)]_t$, the vector of fractions of HCN with $\nu_3=0, 1$, or 2 at time t . The solution is

$$\mathbf{N}_t = \mathbf{N}_0 \exp(\Gamma t), \quad (18)$$

which can be inverted to recover the population at time $t=0$ from that at time t . Γ is the relaxation matrix

$$\Gamma = \begin{pmatrix} -A_{002} - k_{002}[\text{H}_2] & 0 & 0 \\ A_{002} + k_{002}[\text{H}_2] & -A_{001} - k_{001}[\text{H}_2] & 0 \\ 0 & A_{001} + k_{001}[\text{H}_2] & 0 \end{pmatrix} \quad (19)$$

$A_{00\nu_3}$ is the spontaneous emission rate and $k_{00\nu_3}$ is the deactivation rate constant for $(00r_3) \rightarrow (0, 0, r_3 - 1)$. Inserting the observed¹⁸ Einstein coefficient $A_{001} = 74.1\text{ sec}^{-1}$, $k_{001} = 200\text{ Torr}^{-1}\text{ sec}^{-1}$, $[\text{H}_2] = 0.5\text{ Torr}$ and $t = 0.6\text{ msec}$, with $A_{002} = 2A_{001}$ and $k_{002} = 2k_{001}$ (assuming the harmonic oscillator approximation) gives the corrected value $N(002)/N(001) = 0.12\pm 0.03$. As expected, the correc-

tion is on the order of 10%. It is also within the error bounds of the measurements.

Although the relative amounts of $\nu_3=1$ and $\nu_3=2$ can be determined, the probabilities remain unknown as long as no information on the level with $\nu_3=0$ exists. In order to determine some limits for the probabilities, the total emission signal from HCN produced by $\text{CN}^- + \text{HCl}$ was compared to the total emission signal from HCl formed by the reaction $\text{Cl}^- + \text{HBr}$. This was accomplished by changing only the precursor and adjusting the emission current such that the same ion current could be measured at the Faraday plate for each ion. The ratio of total emission from these two sources was 1.

We can write this ratio of intensities as

$$\frac{I(\text{CN}^- + \text{HCl})}{I(\text{Cl}^- + \text{HBr})} = \frac{N(001)A(001) + N(002)A(002)}{N(1)A(1)} \quad (20)$$

or

$$= \left\{ \frac{P(1, \text{CN}^- + \text{HCl}) + P(2, \text{CN}^- + \text{HCl})[A(002)/A(001)]}{P(1, \text{Cl}^- + \text{HBr})} \right\} \times \frac{A(001)}{A(1)}$$

Here, $P(1, \text{CN}^- + \text{HCl})$ is the probability of forming HCN with $\nu_3=1$. Employment of $A(001) = 74.1\text{ sec}^{-1}$ for HCN and $A(1) = 34.6\text{ sec}^{-1}$ for HCl, produces a ratio of 2.14 for the Einstein coefficients. Using $A(002)/A(001) = 2$ and inserting $P(2, \text{CN}^- + \text{HCl}) = 0.12 P(1, \text{CN}^- + \text{HCl})$, we obtain

$$\frac{P(1, \text{CN}^- + \text{HCl})}{P(1, \text{Cl}^- + \text{HBr})} = 0.37 \quad (21)$$

The reactions of chloride ions with HBr and HI have been studied earlier in this apparatus.¹⁷ In a manner analogous to Eq. (20), $P(1, \text{Cl}^- + \text{HBr})/P(1, \text{Cl}^- + \text{HI})$ was found to be 0.96. $P(1, \text{Cl}^- + \text{HBr})$ is the probability of forming HCl ($\nu=1$) by the reaction of Cl^- with HBr. From an extrapolation of a surprisal plot, the probabilities $P(0, \text{Cl}^- + \text{HI}) = 0.21$, $P(1, \text{Cl}^- + \text{HI}) = 0.43$ and $P(2, \text{Cl}^- + \text{HI}) = 0.36$ were obtained. This set of probabilities implies $P(1, \text{Cl}^- + \text{HBr}) = 0.41$. As an extreme case, we could ignore the surprisal analysis and choose $(0, 0.54, 0.46)$ as the vibrational distribution of HCl formed from $\text{Cl}^- + \text{HI}$ rather than $(0.21, 0.43, 0.36)$. This produces an upper limit for $P(1, \text{Cl}^- + \text{HBr})$ of 0.52.

This indicates an uncertainty in our probabilities of $\pm 25\%$.

We can now use these earlier Cl⁻ results to interpret our CN⁻ reactions. If the surprisal value is retained for $P(1, \text{Cl}^- + \text{HBr})$, we use Eq. (21) to find $P(1, \text{CN}^- + \text{HCl}) = 0.15$. The complete distribution is then $P(0, \text{CN}^- + \text{HCl}) = 0.83$, $P(1, \text{CN}^- + \text{HCl}) = 0.15$ and $P(2, \text{CN}^- + \text{HCl}) = 0.02$. These results are prone to error from the measured ratio of total intensities, the neglect of CNH(000), and from the earlier analysis of the Cl⁻ reactions. A reasonable error to assign those probabilities is $\pm 25\%$.

Experiments with argon as the carrier gas were also undertaken. They resulted in a change of the ratio of intensities with and without the cold gas cell to $I_g/I_e = 0.8 \pm 0.1$. The increase from the previous value of 0.19 implies that the HCN molecules with $\nu_3 = 1$ are usually accompanied with excitation in the bending mode. Instead of Eq. (15), a more complicated expression must be used for the intensity ratio

$$\frac{I_g}{I_e} = \frac{A(002)N(002) + \Sigma A(0k1)N(0k1)}{A(001)N(001) + A(002)N(002) + \Sigma A(0k1)N(0k1)}$$

We conjecture that the spontaneous emission coefficient is the same for $(0k1) \rightarrow (0k0)$ as for $(001) \rightarrow (000)$. If $\Sigma N(0k1)$ is referred to as $N(0n1)$, we have

$$\frac{N(0n1)}{N(001)} = \left[\frac{N(002)}{N(001)} \left(\frac{I_g}{I_e} - 1.0 \right) A(2) + \frac{I_g}{I_e} \right] \left(1.0 - \frac{I_g}{I_e} \right)^{-1} \quad (22)$$

Inserting the value $N(002)/N(001) = 0.12$ we see that $N(0n1)/N(001) = 4 \pm 2$. This is rather interesting: 4/5 of the HCN formed with one quantum in ν_3 also have at least one quantum in ν_2 . It seems quite likely then that a similar fraction of HCN with $\nu_3 = 0$ would also have $\nu_2 > 0$. In other words, about 80% of the HCN formed by $\text{CN}^- + \text{HCl}$ will have some excitation in the bending mode.

C. Relaxation of HCN(0n0)

While dealing with Reaction (3), a discussion of the relaxation of HCN(0n0) is in order. It is useful to compare the relaxation properties of HCN to another triatomic molecule about which a great deal is known, CO₂.

Measurements of I_g/I_e were made at distances of 11 and 5 cm from the neutral inlet to the IR detector with H₂ + He, He, and Ar as the carrier gas. A value of $I_g/I_e = 0.8 \pm 0.1$ was obtained at each distance when the collision partner was argon. This allows an upper bound for the rate constant to be obtained by assuming that the maximum fraction deactivated is given by 0.7/0.9 (the worst case within the error limits). With $t = 1.0$ ms and Ar = 0.3 Torr, the upper limit for the rate constant [Eq. (10) with $M = \text{Ar}$] is $k_{\text{Ar}} < 1000 \text{ Torr}^{-1} \text{ sec}^{-1}$ at $T = 295$ K. This may be compared to the value of k_{010} for CO₂ = $26 \text{ Torr}^{-1} \text{ sec}^{-1}$.⁴²

At the other extreme, with the carrier gas a mixture of 0.1 Torr H₂ and 0.4 Torr He, $I_g/I_e = 0.19 \pm 0.02$ at each distance. Thus, all of the energy in the bending mode has been removed in 0.6 msec. This time a lower limit of the rate constant can be obtained [Eq. (10) with

$M = \text{H}_2$]. Assuming that, with the 11 cm distance, 95% of the bending mode has been deactivated yields $k_{\text{H}_2} > 2 \times 10^4 \text{ Torr}^{-1} \text{ sec}^{-1}$; compare with $k_{010} = 4 \times 10^4 \text{ Torr}^{-1} \text{ sec}^{-1}$ for the (VT) deactivation of CO₂(01¹0) by hydrogen.^{42,43}

Helium deactivates HCN(0n1) at a rate intermediate to these two. The intensity ratios through the cold gas filter were as follows: for 0.5 Torr He $I_g/I_e = 0.25 \pm 0.02$ at 11 cm, 0.37 \pm 0.04 at 5 cm and for 0.27 Torr $I_g/I_e = 0.26 \pm 0.04$ at 11 cm, 0.57 \pm 0.05 at 5 cm. Note that the values at 11 cm are reasonably close to 0.19. In fact, were they used in Eq. (15), the results would be $N(2)/N(1) = 0.17$ and $N(2)/N(1) = 0.18$, respectively; not very different from the actual value. The values obtained at 5 cm are treated as described for the argon case. Equation (22) is used giving $N(0n1)/N(001) = 0.35 \pm 0.1$ for 0.5 Torr He and $N(0n1)/N(001) = 1.1 \pm 0.3$ for 0.27 Torr He. The rate constant can then be extracted from

$$\ln \left[\frac{N(0n1)/N(001) \text{ in He}}{N(0n1)/N(001) \text{ in Ar}} \right] = -k[\text{He}]t$$

At both helium pressures the result is within the error bounds of $k_{\text{He}} = 7 \pm 4 \times 10^3 \text{ Torr}^{-1} \text{ sec}^{-1}$. The corresponding deactivation rate for CO₂ is $k_{010} = 3.5 \times 10^3 \text{ Torr}^{-1} \text{ sec}^{-1}$.⁴² Hence, while the results for HCN are approximate, they are in keeping with the prediction that CO₂ would be useful as a guide.

D. CN⁻ + HBr

Owing to the larger exothermicity of the reaction, the maximum quantum number for the C-H stretch is $\nu_3 = 3$, 14 for the bending mode, and 4 for the C \equiv N stretch; the total number of states is 344. Note also Fig. 6. In the hydrogen-helium gas mixture the ratio $I_g/I_e = 0.65 \pm 0.05$ is measured with the cold gas filter. Substituted into Expression (15), this gives $N(002)/N(001) = 1.1 \pm 0.1$. This is not quite correct as excitation to $\nu_3 = 3$ is just possible. To check for this, fixed frequency filters were used with the results shown in Appendix B. After the deconvolution procedure discussed above, these results combined with the cold gas filter results yield the ratios $[N(001):N(002):N(003)] = [0.51:0.44:0.05]$. Errors for these values are $\pm 10\%$. From this we see that when the extra energy is available, the population of $\nu_3 = 2$ is just as likely as for $\nu_3 = 1$. It is interesting to note that, as in the HCl reaction, a small fraction of the HCN is formed with practically all of the exothermicity contained in the newly formed C-H bond.

The cold gas filter has almost no effect when the reaction is run in argon. A ratio of $I_g/I_e = 0.95 \pm 0.05$ is measured. Equation (22) then gives $N(0n1)/N(001) = 13 \pm 10$, the large error resulting from the denominator being close to zero in Eq. (22). This shows that even more so than for the HCl reaction, the majority of the product HCN is born with some excitation in the bending mode.

E. CN⁻ + HI

The larger exothermicity of 12800 cm^{-1} drastically increases the number of available states in the product

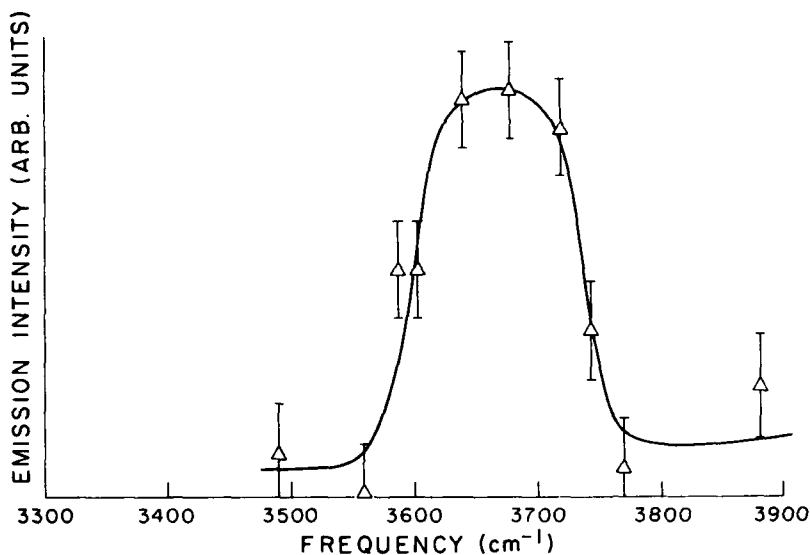
OBSERVED HIGH FREQUENCY EMISSION
FROM REACTION: $\text{CN}^- + \text{HI}$ 

FIG. 7. The results of a point-by-point scan through the high frequency emission spectrum seen in Reaction (5), confirming the assignment as $\text{CNH}(\nu_3)$ emission.

HCN . Roughly 880 vibrational states are accessible. In addition to excitation of HCN , reference to Fig. 6 suggests to us that excited states of CNH may be produced as well. The difference between the zero point energies of those isomers is not certain but, as mentioned above, several computations estimate it at about 5200 cm^{-1} . This implies that about 7600 cm^{-1} are available for excitation of CNH . Under conditions where ν_1 and ν_2 are deactivated, only five states of HCN are left: (000), (001), (002), (003), and (004). Based on the zero point separation of CNH from HCN (ΔE in Fig. 6), (001) and (002) of CNH must be considered for Reaction (5).

The first experiments with HI gave strong evidence for the presence of CNH as a reaction product. When CN^- is mixed with HI in the flow tube, very strong emission is observed when filter WO2644 (see Appendix B) is used. Much weaker signals are found when filter Type 1#4 is employed. Appendix B reports that the latter signal is only about 30% of the former. Appendix B indicates that the essential difference between the filters is that WO2644 transmits light from 3270 up to about 4500 cm^{-1} . It is strongly suggested that we are producing molecules which have high frequency modes emitting in the range 3400 to 4500 cm^{-1} . Very few C-H stretches occur at such high frequencies. The possibility of emission from an O-H stretch (in H_2O or some alcohol) can be dismissed since there is no reason why such a mechanism would occur with only the HI reaction. HCN has no excited electronic states accessible at these energies. The cyano radical CN does have a low lying $^2\Pi$ state,³⁰ but it is endothermic to form it as a product in these ion reactions. If $\text{CN}(^2\Pi)$ were formed by detachment of CN^- at the ion shutter, then the emission would be present for all the reactions. These high frequency signals are observed when either BrCN or C_2N_2 is the CN^- precursor.

We believe that this high frequency emission is from

vibrationally excited CNH . Table III indicates that the N-H stretch is at 3652.9 cm^{-1} . A frequency such as this is entirely consistent with our observations. Two further experiments establish CNH as the carrier of this signal. The first is the direct observation of hydroisocyanic acid with a Ge:Cu IR detector. The second experiment is the direct observation of emission of CND when CN^- is added to DI .

We can replace our InSb detector and its fixed frequency filter with a background limited Ge:Cu detector. This device is housed in a liquid helium Dewar and configured with wavelength selective circular variable interference filters. The high frequency radiation produced by CN^- and HI was monitored with this scanning detector and the resulting emission spectrum is shown in Fig. 7. The peak in the chemiluminescent signal is about 3650 cm^{-1} —precisely the frequency of $\text{CNH}(001)-(000)$. Even though the resolution of the circular variable filters is about 80 cm^{-1} , this signal is easily separated and distinct from the region of ν_3 emission of HCN (3300 – 2900 cm^{-1}).

If CNH is being produced, we should observe an isotope effect. Table III indicates that the (001)–(000) transition of DCN is at 2630 cm^{-1} but is shifted in CND to 2780 cm^{-1} . We have experimentally observed this shift. If we add CN^- to DI in the flow tube and search for emission with an InSb detector and the fixed frequency filter NO3462 (bandpass 2984 – 2799 cm^{-1}), we see a signal. This is shown in Fig. 8. Notice that this filter will completely block all signals from DCN . Figure 8 clearly shows emission from the $\text{CN}^- + \text{DI}$ reaction. This is consistent with the isotope shift predicted for CND . There are at least two reasons why the signal in Fig. 8 is so weak. The first is that our filter NO3462 only transmits a fraction of the R branch of the band. An additional factor is the decrease in the Einstein A factor of CNH upon isotopic substitution. The ratio of

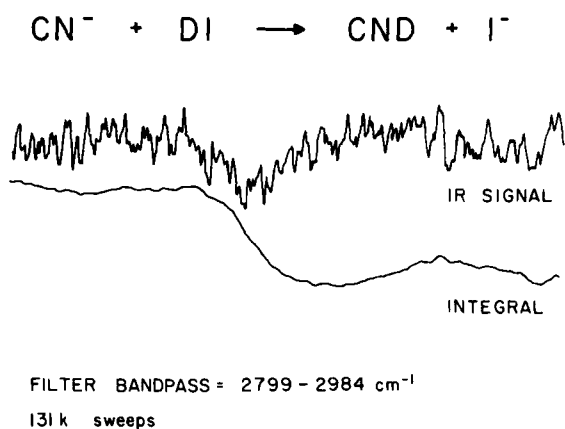


FIG. 8. Emission signal from CND (ν_3) following 10 min of signal averaging.

the A factor for CND to that for CNH should be about $(2780/3652)^3$ or 0.4. Both the frequency and intensity of the signal shown in Fig. 8 are consistent with CND emission.

Measurements of the intensities of emission signals were made with a cold gas filter and four fixed frequency filters; the results are collected in Appendix B. Even with H_2 to deactivate the bends, the cold gas filter ratio was high: $I_g/I_e = 0.9 \pm 0.06$. Part of the reason for this may lie with the possibility of putting up to 19 quanta into ν_2 , with H_2 unable to complete the sequential processes such as $(0, 18, 0) + \text{H}_2 \rightarrow (0, 17, 0) + \text{H}_2$, etc., in the time available. To invert the observed intensities from $\text{CN}^- + \text{HI}$ listed in Appendix B, we use our estimate that A_{CNH} is about four times greater than A_{HCN} . An additional, necessary datum is that $T(\text{WO2644}, \text{CNH}) = 0.73$. We find the following relative populations for the HI reaction:

$$[N(--1): N(--2): N(--3): N(--4): N(\text{CNH})] \\ = [0.21: 0.47: 0.11: 0.02: 0.19].$$

Partly due to the sensitivity of the numbers on the cold gas filter ratio, the error bounds are given as $\pm 40\%$.

F. $\text{CN}^- + \text{H}$

Reaction (6) has been studied before.⁴⁷ The exothermicity for this reaction is roughly the same as for $\text{CN}^- + \text{HI}$. Consequently about the same number of states are available to the reaction products as in the previous section. Surprisingly enough, we find no evidence for vibrationally excited CNH as a reaction product of this associative detachment reaction. The intensity ratios for a set of filters are reported in Appendix B. A deconvolution of these fixed frequency filters and cold gas cell results gave the relative populations

$$[N(--1): N(--2): N(--3): N(--4)] \\ = [0.47: 0.39: 0.09: 0.05].$$

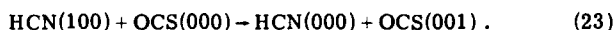
As in the HI reaction, the error bars are large and on the order of $\pm 30\%$.

Attempts to determine the excitation in the bending manifold by running the experiment in argon did not give satisfactory results. The main problems stemmed from the lack of knowledge about the amount of H_2 entering the flow tube through the atom generator and of the deactivation rate of HCN by hydrogen atoms.

G. Energy transfer to OCS

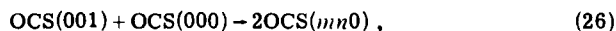
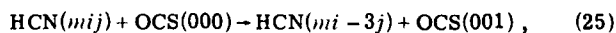
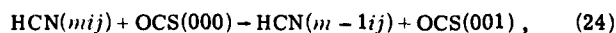
An unknown in these experiments is the state of the $\text{C}\equiv\text{N}$ stretch ν_1 in the product HCN. Since emission from this mode is nil, we have no chance to observe it in fluorescence. Dark modes such as this may be commonly encountered as we study more complicated polyatomic molecules. We need another avenue to detect weak modes. One possible method is to collisionally transfer energy to a bright emitter, as for example in Reaction (23), where OCS is used as an acceptor.

The idea is this:



OCS was chosen for several reasons. The asymmetric stretch of OCS is at $\nu_3 = 2062.2 \text{ cm}^{-1}$; this is only 34 cm^{-1} below the $(100) \rightarrow (000)$ transition frequency in HCN. The small energy defect makes it likely that the rate constant for energy transfer from HCN to carbonyl sulfide will be quite fast. The rate constant⁴⁸ for $V \rightarrow V$ transfer from $\text{CO}(r=1)$ to $\text{OCS}(001)$ is $2.57 \times 10^5 \text{ Torr}^{-1} \text{ s}^{-1}$ at 300 K. Energy equilibration in vibrationally excited OCS has been thoroughly studied.^{49,50} In order to accomplish the transfer from HCN in the 1 ms our flow tube allows, a $V \rightarrow V$ rate constant of roughly $k_{23} = 5 \times 10^3 \text{ Torr}^{-1} \text{ sec}^{-1}$ or greater is required. OCS is an extremely bright emitter ($S_3 = 2634 \text{ atm}^{-1} \text{ cm}^{-2}$) so even if a fraction of the energy is transferred, emission should be observed from the OCS.

The following reactions are important in this scheme:



Collisional equilibration as in Eq. (9) is crucial to this discussion. As already stated, k_{24} should be large. Because the energy defect is also small for Reaction (25), 38 cm^{-1} , this too might be rapid. Hence, it will not be possible to determine whether the energy transferred to the OCS originated from the $\text{C}\equiv\text{N}$ stretch or from the bending mode. The rate constant for the self-relaxation of OCS has been measured⁴⁸ and is fast; $k_{26} = 4.7 \times 10^4 \text{ Torr}^{-1} \text{ sec}^{-1}$. This limits the amount of OCS which can be added to the flow tube to about 10 mTorr. At this pressure 35% of the energy placed into OCS will be deactivated by Reaction (26) by the time the molecules reach the detector. Hancock *et al.*⁴⁸ have measured the rate constant for deactivation of OCS by Ar to be $1.4 \times 10^3 \text{ Torr}^{-1} \text{ sec}^{-1}$. If we assume the same rate constant as for He, this means that 50% of the $\text{OCS}(001)$ will have been lost due to helium collision before detection.

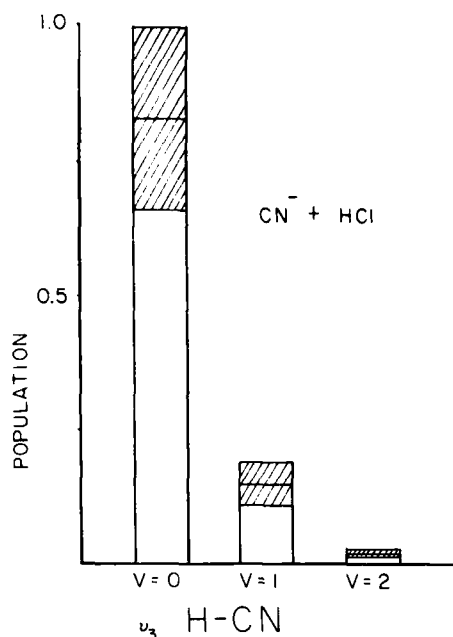


FIG. 9. A histogram of the product distribution for the ν_3 mode of HCN produced by Reaction (3). The hatched areas indicate the error bars.

Even though the rate constants k_{24} and k_{25} were unknown and though $\frac{3}{4}$ of the OCS would be deactivated before we had a chance to observe emission, the experiment was tried. CN^- and HBr alone were combined in the flow tube in view of a filter which accepted light from both HCN(100) and OCS(001). No emission was observed. Addition of 10 mTorr of OCS 10 cm upstream from the InSb detector led to a moderate amount of IR emission. Use of a cold gas cell filled with 25 Torr of OCS blocked emission completely, demonstrating that the emitter is OCS(001). If CN^- is added to the flow tube together with OCS but no HBr, no IR emission is seen. By varying the H_2 pressure in the buffer gas from 0 to 150 mTorr, we can make a crude estimate of $1 \times 10^4 \text{ Torr}^{-1} \text{ sec}^{-1}$ for the rate constant of the quenching Reaction (12). These experiments prove that we can collisionally transfer energy from the product HCN to OCS and detect it.

Is the energy transfer specific? Can we prove that the donating species is HCN(100) and not HCN(030)? The answer is that our results are ambiguous; these transfer experiments cannot distinguish donation by HCN ν_1 from HCN $3\nu_2$. We cannot be sure if Eq. (9) equilibrates the manifolds or not.

If we add 10 mTorr H_2 to the $\text{CN}^- + \text{HBr}$ reaction zone 10 cm upstream from OCS addition, all OCS emission is quenched. Now the process



has a measured⁵¹ collision number of 126 000. It is evident that H_2 is not relaxing the OCS(001), but is quenching the vibrationally excited HCN formed by the reaction. Consequently it appears that if Eq. (9) equilibrates ν_1 with ν_2 , both modes are relaxed by the H_2 . If Eq. (9) does not equilibrate the modes, then no $\text{HCN}(v--)$ is a reaction product.

V. DISCUSSION

The major fact to emerge from this work is that it has been possible to study the energy distribution in a polyatomic molecule born in an ion-molecule reaction. It is apparent that the excess vibrational energy does not become scrambled among the available vibrational modes while the reactants pass through the deep potential well separating reactants and products. We have been able to derive information on the degree of excitation of the product HCN in the ν_3 manifold. Unfortunately, we can say very little about the energy distribution in the other modes except that a considerable number of bending quanta must be excited (ν_2).

A comparison between the total IR intensity emitted by the reactions $\text{CN}^- + \text{HCl}$ and $\text{Cl}^- + \text{HX}$ has demonstrated that a high fraction of the HCN is produced in the ($\nu_3 = 0$) state (see Sec. IV B). A histogram of this nascent distribution is shown in Fig. 9. This analysis does not depend upon the accuracy of a surprisal plot based on a very limited amount of data. Table IV collects the relative product HCN distributions resulting from the $\text{CN}^- + (\text{HCl}, \text{HBr}, \text{HI}, \text{and } \text{H})$ reactions. These are the nascent distributions for the C-H stretching mode ν_3 . A histogram of these data is presented in Fig. 10. Naturally, we have no direct measure of the $\nu_3 = 0$ population. As one goes from the case of HCl, to HBr, to HI and H, the reactions become more exothermic (see Table I) and the product distributions become hotter. As remarked earlier, each reaction produces some fraction of the HCN product molecules excited to the highest level in the ν_3 ladder which is energetically accessible. It is apparent that the vibrational energy distribution in the HCN is not random.

In the previous studies of Cl^- or F^- dynamics,^{17,52,53} angular momentum restrictions markedly affected the distributions in the associative detachment reactions $\text{Cl}^- + \text{H} \rightarrow \text{HCl}(v)$ or $\text{HF}(v) + e^-$. In both cases, most of the angular momentum associated with the in-

TABLE IV. Relative product distributions for CN^- reactions.

Reaction	H-CN (ν_3)			P (4)	CN-H (ν_3)
	P (1)	P (2)	P (3)		P (1)
$\text{CN}^- + \text{HCl}$	0.89 ± 0.03	0.11 ± 0.03
$\text{CN}^- + \text{HBr}$	0.51 ± 0.05	0.44 ± 0.05	0.05 ± 0.02
$\text{CN}^- + \text{HI}$	0.21 ± 0.10	0.47 ± 0.13	0.11 ± 0.06	0.02 ± 0.02	0.19 ± 0.05
$\text{CN}^- + \text{H}$	0.47 ± 0.05	0.39 ± 0.10	0.09 ± 0.04	0.05 ± 0.03	0.0 ± 0.05

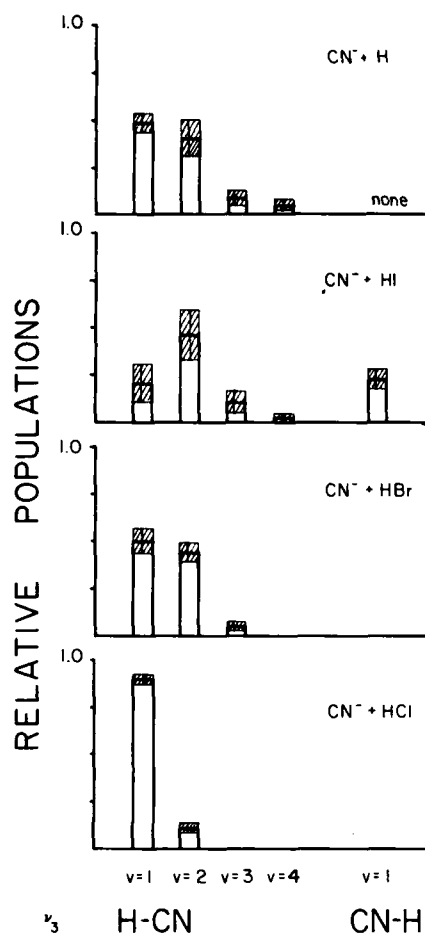


FIG. 10. A histogram of the observed product distributions (Table IV) for the ν_3 modes of HCN and CNH in Reactions (3)–(6). The hatched areas are indications of the errors in these distributions. Each distribution is normalized to 1.0 ignoring population in the $\nu=0$ states.

coming particles was lodged in the product HX molecules as rotation. The large rotational spacings³⁰ for HF and HCl require that this obligatory rotational energy is a significant portion of the reaction energy available. In both reactions, the vibrational energy distributions of the product HF and HCl molecules manifest a noticeable truncation of the higher ν 's excited.

Both HCl and HF are unusual molecules with large rotational constants.³⁰ HCN is more typical with a B_r of about 1.5 cm^{-1} (Table III). Consequently, in Reaction (6), angular momentum restrictions require only roughly 275 cm^{-1} of energy to be placed in rotation. This is a rather small portion of the total energy available to HCN ($12\,800 \text{ cm}^{-1}$), so there is no distortion of the product vibrational distribution.

A second important and unexpected result of these studies is the detection of CNH, produced in the reaction of CN^- with HI. In fact, CNH represents roughly 20% of the excited product molecules formed in Reaction (5).

As implied in Fig. 10, our experiments allow us to

place bounds on the zero point energy difference between HCN and CNH (shown in Fig. 6 as ΔE). Since we observe vibrationally excited CNH as a reaction product from $\text{CN}^- + \text{HI}$ but not from $\text{CN}^- + \text{HBr}$, ΔE must be less than 9200 cm^{-1} . This number is based on the reaction exothermicity of Reaction (5) and the 3600 cm^{-1} necessary to excite CNH from (000) to (001). In contrast, Reaction (4) does not seem to be exoergic enough to generate CNH ($\nu_3=1$); so ΔE is probably greater than 6000 cm^{-1} . Our conjecture is, then, $6000 \text{ cm}^{-1} < \Delta E < 9200 \text{ cm}^{-1}$. The only other value reported³⁴ for ΔE is 3670 cm^{-1} , much lower than our estimate. However, our bounds are in reasonable agreement with *ab initio* theoretical values^{32,33} for ΔE of about 5200 cm^{-1} .

The rearrangement or isomerization of CNH to HCN has been the subject for a great deal of theoretical study. Many groups have computed potential surfaces for these isomeric species^{32,33,54} and several trajectory studies⁵⁵ have been made of the isomerization dynamics. Another unlikely fact to emerge from our experiments is that $\text{HCN}(\nu=4)$ does not equilibrate with CNH. Table IV and Fig. 10 report that $\text{HCN}(\nu=4)$ is produced by $\text{CN}^- + \text{H}$, Reaction (6). Once HCN is born with $\nu=4$, it remains in the HCN well; no excited CNH is detected. This suggests that the barrier separating CNH from HCN is greater than 6600 cm^{-1} . This value comes from our minimum ΔE (6000 cm^{-1}) and the energy of HCN (004) ($12\,600 \text{ cm}^{-1}$). A barrier height of about $10\,500 \text{ cm}^{-1}$ has been theoretically calculated for this separation.^{32,33} This value is consistent with our observations.

The formation of CNH, an interstellar molecule, by a negative ion-molecule reaction is most provocative. As mentioned earlier, hydroisocyanic acid has been observed in the Orion Nebula by radio emission.^{22,56–58} Several of the postulated schemes to synthesize CNH in outer space are based on positive ion reactions.⁵⁹ No proposals for CNH production based on negative ions have yet been made. Although we now have a proven case for CN^- as a CNH precursor, our only example involves HI. For CN^- to be implicated in interstellar CNH production, Reaction (6) with hydrogen atoms may be decisive. We find no evidence that Reaction (6) produces CNH, even though it is certainly exothermic enough to do so (Table I). Conceivably, Reaction (6) could yield $\text{CNH}(\nu=0)$, but it seems unlikely to us that there would be absolutely no accompanying $\text{CNH}(\nu=1)$. If CN^- is to react with something in the interstellar medium to produce CNH, H is the best bet, not HI.⁵⁸ It appears that reactions of CN^- probably are not important in the synthesis of astrophysical CNH.⁶⁰

The reason for the failure of $\text{CN}^- + \text{H}$ to yield $\text{CNH}(\nu)$ is not clear. Since we see emission from $\text{HCN}(\nu=4)$, we know that Reaction (6) has enough energy to form both isomers. One speculative mechanism that may account for the lack of $\text{CNH}(\nu)$ production in Reaction (6) can be borrowed from Fehsenfeld⁴⁷ and is shown in Fig. 11. We could imagine that $\text{CN}^- + \text{H}$ may form a negative ion (HCN^-) which is stable enough to enter the autodetaching region (curve II in Fig. 11). On the other hand, if $\text{CN}^- + \text{H}$ forms the isomeric ion (CNH^-) it may not be stable enough to enter the autodetaching

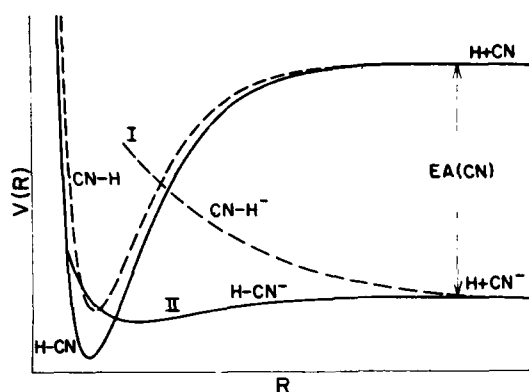


FIG. 11. A conjectured set of potential curves to describe the associative detachment reaction $\text{CN}^- + \text{H} \rightarrow \text{HCN}(\nu_3) + e^-$. CN^- combining with H to form $(\text{HCN})^-$ follows the solid curve II into the autodetaching region where it is unstable with respect to HCN and a free electron. CN^- combining with H to form $(\text{CNH})^-$ may follow the dashed curve I. $(\text{CNH})^-$ is never stable enough to reach the autodetaching region; consequently, it cannot produce CNH and a free electron.

region (curve I in Fig. 11). We have no evidence that supports or suggests this mechanism so far.

ACKNOWLEDGMENTS

The authors wish to thank the many people who gave advice, criticism, and encouragement to this project. These included V. M. Bierbaum, S. R. Leone, T. S. Zwier, D. J. Nesbitt, C. J. Howard, F. C. Fehsenfeld, J. C. Weisshaar, C. H. DePuy, and S. A. Sullivan. We have relied on the friendly help of the staff of the JILA workshops and are indebted to Dr. J. J. Wendoloski of the NRCC for the CNH dipole moment derivative calculation. Thanks are due to Leslie Haas for typing a vexing manuscript several times. The authors gratefully acknowledge the support of the Air Force Office of Scientific Research. M. M. M. thanks the Army Research Office for support and C. J. S. M. S. the Science Research Council for a Senior Visiting Fellowship. G. B. E. is a Fellow of the Alfred P. Sloan Foundation.

APPENDIX A

1. Overtone A factors for HCN

We must have values for the ratios of Einstein A factors in order to find the relative populations of emitting states. $A(001-000)$ has been measured¹⁸ to be 74.1 sec^{-1} but others, $A(002-001)$ etc., are not available.

TABLE V. Ratios of HCl Einstein coefficients.

Transition	μ_{ij} (esu cm)	ν_{ij} (cm^{-1})	A ratio	Estimated ratio
1-0	7.12(-20)	2887.0
2-1	9.93(-20)	2782.6	1.74	1.79
3-2	11.93(-20)	2679.3	2.24	2.40
4-3	13.40(-20)	2576.8	2.52	2.84

TABLE VI. Estimated A ratios for HCN.

Transition	Observed ν_{ij} (cm^{-1})	Harmonic transition moments	A (ν)
(001) \rightarrow (000)	3311.4	1	...
(002) \rightarrow (001)	3206.4	2	1.82
(003) \rightarrow (002)	3101.4	3	2.46
(004) \rightarrow (003)	2996.5	4	2.96

This Appendix describes a recipe for estimating the ratios we need

$$A(\nu_3) = A[(\nu_3) - (\nu_3 - 1)] / A[(\nu_3 = 1) - (\nu_3 = 0)].$$

The Einstein A factor is, essentially, a product of a frequency factor and a dipole matrix element⁶²

$$A_{10} = \frac{4}{3h} \left(\frac{2\pi}{c} \right)^3 \nu_{10}^3 |\langle 000 | \mu | 001 \rangle|^2. \quad (\text{A1})$$

In this expression, ν is the transition frequency and μ is the dipole moment operator. Recall that for the case of an harmonic oscillator, the ratios $A(\nu_3)$ defined in Eq. (13) become $A(1)=1$, $A(2)=2$, $A(3)=3$, and $A(4)=4$. This is not a reasonable procedure to follow when treating real, anharmonic molecules. We wish to explore a method that uses the experimental transition frequencies ν and approximates the dipole matrix elements μ_{1m} with harmonic values. An application of this method to HCl is illuminating. Table V lists the observed transition moments⁶⁴ and frequencies up to $\nu=4$. The ratios of the experimental A coefficients⁶⁴ are listed in the column A ratio. The last entry has the estimated ratios. As an example, we approximate the A_{32}/A_{10} ratio as $(2679.3/2887.0)^3 \times 3$ or about 2.40. This is within 7% of the observed ratio.

Let us employ this procedure to estimate the ratios of Einstein coefficients for the ν_3 manifold of HCN. We use the observed transition frequencies³⁵ and harmonic matrix elements. These ratios are entered as the last column of Table VI. The final values we will use in Eq. (13) to deconvolute our HCN experiments are: $A(2)=1.82$, $A(3)=2.46$, and $A(4)=2.96$. We estimate that these ratios may be in error by $\pm 10\%$.

2. The CNH A factor

We wish to know how bright an infrared emitter CNH is. Experimental intensities are not available for this reactive species. We can estimate these in the following manner. Wilson, Decius and Cross⁶² write the absorption strength between two states $|0\rangle$ and $|1\rangle$ as

$$S = \frac{8\pi^3}{3ch} N_0 \nu_{10} |\mu_{10}|^2. \quad (\text{A2})$$

In this expression, N_0 is the number density of absorbing molecules in state $|0\rangle$, ν_{10} is the transition frequency, and μ_{10} is the transition moment matrix element.

For a transition involving a nondegenerate normal mode Q_n expression (A2) can be approximated by

$$S \sim \frac{N_0 \pi}{3c} \left(\frac{\partial \mu}{\partial Q_n} \right)_0^2. \quad (\text{A3})$$

TABLE VII. Interference filter transmission functions $T(f, \nu_3)$.^a

Transition	Filter and (bandwidth cm ⁻¹)			
	WO2644 (4488-3270)	Type 1#4 (3330-3180)	Type 2#15 (3090-2960)	NO3462 (2984-2799)
005 → 004	0.0	0.0	0.01	0.52
004 → 003	0.0	0.0	0.34	0.48
003 → 002	0.01	0.0	0.44	0.05
002 → 001	0.06	0.17	0.04	0.0
001 → 000	0.52	0.52	0.0	0.0

^aThe $T(f, \nu_3)$ are defined in Eq. (14).

We wish to exploit Eq. (A3) to estimate the absorption strength of CNH(000) → (001). Dr. J. J. Wendoloski has evaluated the dipole moment derivatives in Eq. (A3) for both HCN and CNH. This has been carried out with *ab initio* GVB(PP) computer codes. A Gaussian basis set was adopted with sufficient flexibility such that evaluation of the dipole moment derivative for HCN, $(\partial\mu/\partial Q_3)_{\text{HCN}}$, leads to a reasonable value of S_3 (see Table III). With this basis set, the dipole moment derivative for CNH was evaluated. It is found that $(\partial\mu/\partial Q_3)_{\text{CNH}} = 1.8(\partial\mu/\partial Q_3)_{\text{HCN}}$. From Eqs. (A1 and (A3) together with the frequencies from Table III, we can conjecture a relative value for the Einstein A coefficient for CNH(001) → (000), $A_{001}(\text{CNH})/A_{001}(\text{HCN}) = 4.0$.

APPENDIX B

This appendix collects together several of the properties of our fixed frequency filters. The functions $T(f, \nu_3)$, defined in Eq. (14), characterize the filters and are listed in Table VII. Below each filter name is the experimentally determined band pass in cm⁻¹. For example, NO3462 transmits light between 2984 and 2799 cm⁻¹.

Table VIII lists experimentally observed intensities from Reactions (3)–(6). The normalization of emission intensities is arbitrary and varies from reaction to reaction.

TABLE VIII. Observed relative emission intensities.

Reaction	Filter	Relative intensity	Total emission
CN ⁻ + HCl	Cold gas ratio	0.19	1.0
CN ⁻ + HBr	Cold gas ratio	0.65	2.5
	Type 1#4	1.10	
	Type 2#15	0.25	
CN ⁻ + H	Cold gas ratio	0.69	4.2
	Type 1#4	1.08	
	Type 2#15	0.51	
	NO3462	0.24	
CN ⁻ + HI	Cold gas ratio	0.90	2.5
	WO2644	2.80	
	Type 1#4	1.00	
	Type 2#15	0.66	
	NO3462	0.13	

- ¹J. C. Polanyi, *Acc. Chem. Res.* **5**, 161 (1972).
- ²J. M. Farrar and Y. T. Lee, *Annu. Rev. Phys. Chem.* **25**, 357 (1974).
- ³J. P. Toennies, in *Physical Chemistry: An Advanced Treatise*, edited by H. Eyring, D. Henderson, and W. Jost (Academic, New York, 1974), Vol. VIA, Chap. 6.
- ⁴P. M. Maylotte, J. C. Polanyi, and K. B. Woodall, *J. Chem. Phys.* **57**, 1547 (1972).
- ⁵I. W. M. Smith, *Kinetics and Dynamics of Elementary Gas Reactions* (Butterworths, London, 1980).
- ⁶D. L. Albritton, in *Kinetics of Ion-Molecule Reactions*, NATO Advance Study Institute Series, edited by P. Ausloos (Plenum, New York, 1979), Vol. B 40, p. 119.
- ⁷D. L. Albritton, *At. Data Nucl. Data Tables* **22**, 1 (1978).
- ⁸*Gas Phase Ion Chemistry*, edited by M. T. Bowers (Academic, New York, 1979).
- ⁹J. I. Brauman, in *Kinetics of Ion-Molecule Reactions*, NATO Advance Study Institute Series, edited by P. Ausloos (Plenum, New York, 1979), Vol. B 40, p. 153.
- ¹⁰N. M. M. Nibbering, *Ref. 9*, p. 1675.
- ¹¹J. L. Beauchamp, in *Interactions Between Ions and Molecules*, NATO Advance Study Institute Series, edited by P. Ausloos (Plenum, New York, 1975), Vol. B 6, p. 413.
- ¹²P. Kebarle, *Annu. Rev. Phys. Chem.* **28**, 445 (1977).
- ¹³W. R. Gentry, in *Gas Phase Ion Chemistry*, edited by M. T. Bowers (Academic, New York, 1979), p. 221.
- ¹⁴I. Kusunoki and Ch. Ottinger, *J. Chem. Phys.* **70**, 699 (1979) and **73**, 2069 (1980).
- ¹⁵V. M. Bierbaum, G. B. Ellison, J. H. Futrell, and S. R. Leone, *J. Chem. Phys.* **67**, 2375 (1977).
- ¹⁶E. E. Ferguson, F. C. Fehsenfeld, and A. L. Schmeltekopf, *Adv. At. Mol. Phys.* **5**, 1 (1969).
- ¹⁷T. S. Zwier, V. M. Bierbaum, G. B. Ellison, and S. R. Leone, *J. Chem. Phys.* **72**, 5426 (1980).
- ¹⁸A. Hariri, A. B. Petersen, and C. Wittig, *J. Chem. Phys.* **65**, 1872 (1976).
- ¹⁹A. B. Petersen and I. W. M. Smith, *J. Chem. Phys.* **71**, 3346 (1979).
- ²⁰G. P. Arnold, R. P. Fernando, and I. W. M. Smith, *J. Chem. Phys.* **73**, 2773 (1980).
- ²¹G. Roden, Ph.D. thesis, Göttingen, 1975.
- ²²L. E. Snyder and D. Buhl, *Bull. Am. Astron. Soc.* **3**, 388 (1971).
- ²³M. Morris, B. Zuckerman, B. E. Turner, and P. Palmer, *Astrophys. J. Lett.* **192**, L 27 (1974).
- ²⁴L. E. Snyder and J. M. Hollis, *Astrophys. J. Lett.* **204**, L 139 (1976).
- ²⁵K. Ziegler, *Org. Synth.* **1**, 314 (1941).
- ²⁶Halocarbon Wax from Halocarbon Products Corporation, New Jersey.
- ²⁷D. W. Trainor, D. O. Ham, and F. Kaufman, *J. Chem. Phys.* **58**, 4599 (1973).
- ²⁸J. Berkowitz, W. A. Chupka, and T. A. Walter, *J. Chem. Phys.* **50**, 1497 (1968).
- ²⁹D. R. Stull and H. Prophet, *JANAF Thermochemical Tables*, Natl. Stand. Ref. Data Ser. Natl. Bur. Stand. Circular 37, (Washington, D. C., 1971).
- ³⁰K. P. Huber and G. Herzberg, *Molecular Spectra and Molecular Structure, IV. Constants of Diatomic Molecules* (Van Nostrand, New York, 1979).
- ³¹H. Hotop and W. C. Lineberger, *J. Phys. Chem. Ref. Data* **4**, 539 (1975).
- ³²P. K. Pearson, G. L. Blackman, H. F. Schaefer, B. Roos, and U. Wahlgren, *Astrophys. J. Lett.* **184**, L 19 (1973).
- ³³L. T. Redmon, G. D. Purvis III, and R. J. Bartlett, *J. Chem. Phys.* **72**, 986 (1980).
- ³⁴A. G. Maki and R. L. Sams, quoted in *Ref. 33*.
- ³⁵H. C. Allen, Jr., E. D. Tidwell, and E. K. Plyer, *J. Chem. Phys.* **25**, 302 (1956).
- ³⁶K. Kim and W. T. King, *J. Chem. Phys.* **71**, 1967 (1979).

- ³⁷The strength of an absorption S is defined as the integral of the absorption coefficient $k(\nu)$ over the transition bandwidth $S = \int_{\text{band}} k(\nu) d\nu$. If p is the sample pressure and l is the absorption path length, in the limit of $pl \rightarrow 0$, S takes on a simple form $S = (1/pl) \int_{\text{band}} \ln(I_0(\nu)/I(\nu)) d\nu$. Here, $I(\nu)$ is the radiation intensity at frequency ν and S has the units of $\text{atm}^{-1} \text{cm}^{-2}$ or km mole^{-1} .
- ³⁸I. A. Gribov and V. N. Smirnov, *Sov. Phys. Usp.* **4**, 919 (1962).
- ³⁹D. E. Milligan and M. E. Jacox, *J. Chem. Phys.* **39**, 712 (1963).
- ⁴⁰C. A. Arrington and E. A. Ogryzlo, *J. Chem. Phys.* **63**, 3670 (1975).
- ⁴¹R. R. Jacos, K. J. Pattipiece, and S. J. Thomas, *Phys. Rev. A* **11**, 54 (1975).
- ⁴²D. C. Allen, T. Scragg, and C. J. S. M. Simpson, *Chem. Phys.* **51**, 279 (1980).
- ⁴³C. J. S. M. Simpson and T. R. D. Chandler, *Proc. R. Soc. London Ser. A* **317**, 265 (1970).
- ⁴⁴G. Inoue and S. Tsuchiya, *J. Phys. Soc. Jpn.* **38**, 87 (1975).
- ⁴⁵J. A. McGarvey Jr., N. E. Friedman, and T. A. Cool, *J. Chem. Phys.* **66**, 3189 (1977).
- ⁴⁶*The Infrared Handbook*, Optical Coating Laboratory Inc. (Santa Rosa, California, 1970), p. 40.
- ⁴⁷F. C. Fehsenfeld, in *Interactions Between Ions and Molecules*, NATO Advance Study Institute Series, edited by P. Ausloos (Plenum, New York, 1975), Vol. B 6, p. 387.
- ⁴⁸J. K. Hancock, D. F. Starr, and W. H. Green, *J. Chem. Phys.* **61**, 3017 (1974).
- ⁴⁹D. R. Siebert and G. W. Flynn, *J. Chem. Phys.* **64**, 4973 (1976).
- ⁵⁰M. L. Mandich and G. W. Flynn, *J. Chem. Phys.* **73**, 1265 (1980).
- ⁵¹B. M. Hopkins, A. Baronavski, and A. Chen, *J. Chem. Phys.* **59**, 836 (1973).
- ⁵²T. S. Zwier, M. M. Maricq, C. J. S. M. Simpson, V. M. Bierbaum, G. B. Ellison, and S. R. Leone, *Phys. Rev. Lett.* **44**, 1050 (1980).
- ⁵³T. S. Zwier, J. C. Weisshaar, and S. R. Leone (in preparation).
- ⁵⁴J. N. Murrell and A. A. Derzi, *J. Chem. Soc. Faraday II*, **76**, 319 (1980).
- ⁵⁵S. K. Gray, W. H. Miller, Y. Yamaguchi, and H. F. Schaefer III, *J. Chem. Phys.* **73**, 2733 (1980).
- ⁵⁶R. J. Saykally, P. G. Szanto, T. G. Anderson, and R. C. Woods, *Astrophys. J.* **204**, L143 (1976).
- ⁵⁷E. F. Pearson, R. A. Creswell, M. Winnewisser, and G. Winnewisser, *Z. Naturforsch. Teil A* **31**, 1394 (1976).
- ⁵⁸A. P. C. Mann and D. A. Williams, *Nature* **283**, 721 (1980).
- ⁵⁹Several possibilities are discussed in T. L. Allen, J. D. Goddard, and H. F. Schaefer III, *J. Chem. Phys.* **73**, 3255 (1980) or F. W. McLafferty and D. C. McGilvery, *J. Am. Chem. Soc.* **102**, 6189 (1980).
- ⁶⁰Since we find CNH to be produced by the exothermic proton transfer Reaction (5), we should not completely dismiss CN^- as a hydroisocyanic acid precursor. If a species with a high gas phase acidity, see Ref. 61, (say about 315 kcal/mol) is shown to be extant in the interstellar medium, it may well furnish CNH by reaction with CN^- .
- ⁶¹J. E. Bartmess, J. A. Scott, and R. T. McIver Jr., *J. Am. Chem. Soc.* **101**, 6046 (1979).
- ⁶²E. B. Wilson, J. C. Decius, and P. C. Cross, *Molecular Vibrations* (McGraw-Hill, New York, 1955), p. 162.
- ⁶³T. Su and M. T. Bowers, in Ref. 8, p. 83.
- ⁶⁴F. G. Smith, *J. Quant. Spectrosc. Radiat. Transfer* **13**, 717 (1973).

(18) ARO

Unclassified

SECURITY CLASSIFICATION OF THIS PAGE (When Data Entered)

REPORT DOCUMENTATION PAGE		READ INSTRUCTIONS BEFORE COMPLETING FORM
1. REPORT NUMBER 19 16004.7-C	2. GOVT ACCESSION NO. AD-A103 695 N/A	3. RECIPIENT'S CATALOG NUMBER N/A
4. TITLE (and Subtitle) 6 Vibrational Product States from Reactions of CN with the Hydrogen Halides and Hydrogen Atoms	5. TYPE OF REPORT & PERIOD COVERED Reprint	
7. AUTHOR(S) 10 M. Matti/Maricq Mark A. Smith C. J. S. M. Simpson	G. Barney/Elison	8. CONTRACT OR GRANT NUMBER(s) DAAG29-79-G-0012
9. PERFORMING ORGANIZATION NAME AND ADDRESS University of Colorado Boulder, CO 80309	10. PROGRAM ELEMENT, PROJECT, TASK AREA & WORK UNIT NUMBERS N/A	
11. CONTROLLING OFFICE NAME AND ADDRESS U. S. Army Research Office P. O. Box 12211 Research Triangle Park, NC 27709	12. REPORT DATE 1 Jun 81	13. NUMBER OF PAGES 17
14. MONITORING AGENCY NAME & ADDRESS (if different from Controlling Office)	15. SECURITY CLASS. (of this report) Unclassified	
15a. DECLASSIFICATION/DOWNGRADING SCHEDULE		
16. DISTRIBUTION STATEMENT (of this Report) Submitted for announcement only.		
17. DISTRIBUTION STATEMENT (of the abstract entered in Block 20, if different from Report)		
18. SUPPLEMENTARY NOTES		
19. KEY WORDS (Continue on reverse side if necessary and identify by block number)		
20. ABSTRACT (Continue on reverse side if necessary and identify by block number)		

Accession For

NTIS GRA&I
 DTIC TAB
 Unannounced
 Justification

By _____
 Distribution/Availability Codes
 Dist. _____ and/or _____
 Special

A 21

**DAT
ILMI**